

# Simultaneous quantum and classical communication using continuous variable

Bing Qi<sup>1,2,\*</sup>

<sup>1</sup>*Quantum Information Science Group, Computational Sciences and Engineering Division,  
Oak Ridge National Laboratory, Oak Ridge, TN 37831-6418, USA*

<sup>2</sup>*Department of Physics and Astronomy, The University of Tennessee, Knoxville, TN 37996 - 1200, USA*

(Dated: June 28, 2022)

Conventionally, classical optical communication systems employing strong laser pulses and quantum key distribution (QKD) systems working at single-photon levels are quite different communication modalities. Dedicated devices are commonly required to implement QKD. Here we show these two can be implemented simultaneously using the same information carriers. More specially, we propose a coherent communication scheme where both the binary bits for a classical communication protocol and Gaussian distributed random numbers for a QKD protocol are encoded on the *same* weak coherent pulses, and decoded by the same coherent receiver. Simulation results based on realistic system parameters show that both deterministic classical communication with a bit error rate of  $10^{-9}$  and secure key distribution can be achieved over  $30\text{km}$  single mode fibers. It is conceivable that in the future coherent optical communication network, QKD is operated in the background of classical communication at negligible cost.

PACS numbers: 03.67.Dd

## I. INTRODUCTION

One of the most practical applications of quantum information science is the so-called quantum key distribution (QKD) protocol, which allows two remote parties, normally referred to as Alice and Bob, to generate a secure key through an insecure quantum channel [1–5]. The generated secure key can be further applied in other cryptographic protocols to enhance communication security.

In the first QKD protocol, the BB84 QKD protocol [1], information is carried by single-photon signals. Due to the channel loss and other implementation imperfections, those single-photon signals are detected in a probabilistic fashion with a relatively high quantum bit error rate (QBER) in the order of  $10^{-2}$ [6]. This is in sharp contrast to a classical optical communication system, where information can be transmitted deterministically in an almost error-free fashion. Furthermore, specialized devices, such as single photons detector (SPD), are typically required in QKD. This makes QKD a very different communication modality in comparison with classical communication.

More recently, continuous-variable (CV) QKD protocols based on optical coherent detection have been proposed and demonstrated as viable solutions [7–10]. In an optical coherent receiver, a strong laser pulse called local oscillator (LO) is mixed with the incoming quantum signal at a beam splitter. The resulting interference signal is strong enough and can be detected using highly efficient photo-diodes working at room temperature. The strong LO also acts as a natural and extremely selective filter, which can suppress broadband noise photons generated in the communication channel effectively. This intrinsic filtering function is especially useful when conducting

QKD over a noisy channel, such as a lit fiber in a conventional fiber optic network [11, 12] or a free-space optical link [13].

One well-known CV-QKD protocol is the Gaussian-modulated coherent states (GMCS) protocol [9], which has been demonstrated over  $80\text{km}$  telecom fiber [10]. The hardware required for implementing the GMCS QKD is surprisingly similar to that for classical coherent optical communication [14]. In fact, recent progresses in both communities have significantly reduced the gap between them. On one hand, the continuous improvement of detector performance in classical coherent communication allows people to achieve a bit error rate (BER) of  $10^{-9}$  with only a few photons per bit [15]. On the other hand, CV-QKD protocols based on discrete modulation, which are similar to the binary phase-shift keying (BPSK) and the quadrature phase-shift keying (QPSK) schemes in classical communication, have been proposed [16, 17]. In this paper, we show it is possible to implement both classical communication and QKD *simultaneously* using the same communication infrastructure. As a specific example, we propose a coherent communication scheme where both the binary bits for the BPSK protocol and Gaussian distributed random numbers for the GMCS QKD protocol are encoded on the *same* weak coherent pulses, and decoded by the same coherent receiver. Such a scheme could be very appealing in practice, where quantum information for QKD is superimposed on classical communication signals, and secure key distribution is conducted in the background of classical communication. This work is partly inspired by [18], where the authors propose improved schemes to implement CV-QKD using a locally generated LO [19–21]. One scheme proposed in [18] is to estimate the phase difference between two remote lasers by sending Gaussian modulated coherent states displaced in phase space. In our scheme, we encode classical information on the displacement of QKD signals.

\* qib1@ornl.gov

This paper is organized as follows: in Section II, we present details of the proposed protocol. In Section III, we conduct numerical simulations based on realistic system parameters. Finally, we conclude this paper with a brief discussion in Section IV.

## II. DETAILS OF THE NEW PROTOCOL

For simplicity, in this paper we assume the BPSK scheme and the GMCS protocol are adopted in classical communication and QKD, correspondingly. The basic idea should be applicable in other encoding schemes.

### A. Classical coherent communication using BPSK

In the BPSK modulation scheme, the classical binary information is encoded on the phase of a coherent state, and decoded by performing optical homodyne detection. More specifically, the bit value  $m_A$  ( $m_A = 0, 1$ ) is encoded as  $|e^{-im_A\pi}\alpha\rangle$ , as shown in Fig.1(a). Without loss of generality, we have assumed  $\alpha$  is a real number. The average photon number  $\mu$  of the coherent state is given by  $\mu = \alpha^2$ .

We assume that the X-quadrature of the signal is measured by the receiver. The probability density function (PDF) of the measurement result  $x_C$  is shown in Fig.1(a) (right figure). The receiver can decode binary information using the sign of  $x_C$ , i.e., if  $x_C > 0$  ( $< 0$ ), the bit value is assigned as “0” (“1”). The BER of the BPSK scheme is determined by the measurement error variance  $\sigma$  and the signal amplitude  $\alpha$ , and is given by [14]

$$BER = \frac{1}{2} \operatorname{erfc}\left(\frac{\sqrt{T_{ch}\eta}\alpha}{\sqrt{2}\sigma}\right) \quad (1)$$

where  $T_{ch}$  is the channel transmittance,  $\eta$  is the detection efficiency, and  $\operatorname{erfc}(\cdot)$  denotes the complementary error function. If the homodyne detector is shot-noise limited (the technical noise is much lower than the vacuum noise), then  $\sigma$  is about  $1/4$ . From (1), we only need 9 photons per bit at the receiver’s end to achieve a BER of  $10^{-9}$ .

### B. GMCS QKD

In GMCS QKD, Alice prepares coherent states  $|x_A + ip_A\rangle$  and sends them to Bob through an insecure quantum channel. Here  $x_A$  and  $p_A$  are Gaussian random numbers with a mean of zero and a variance of  $V_A N_0$ , where  $N_0 = 1/4$  denotes the shot-noise variance. At Bob’s end, he can either perform optical homodyne detection to measure a randomly chosen quadrature [9], or perform optical heterodyne detection to measure both quadrature [22]. In this paper, our discussion is based on the homodyne detection scheme. The essential ideas

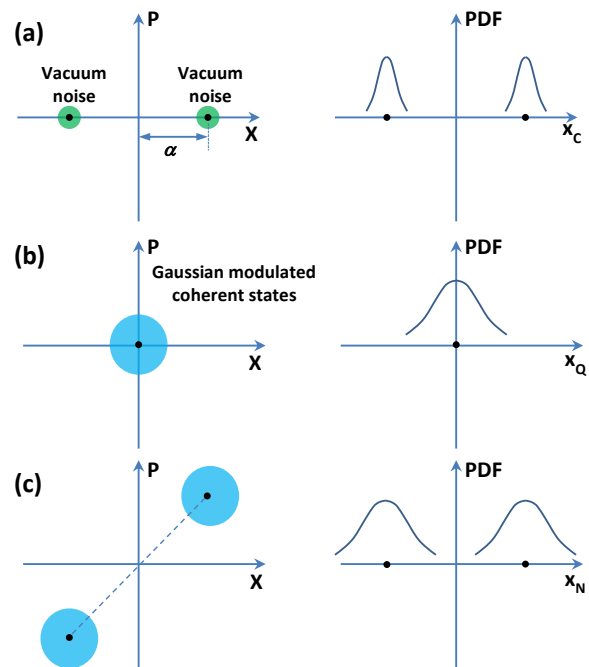


FIG. 1: Phase space representations of various modulation schemes. (a) BPSK modulation scheme. (b) GMCS modulation scheme. (c) the proposed modulation scheme. The figures on the right show the probability density functions (PDF) of X-quadrature measurement results.

can be extended to the other case. Fig.1(b) shows the phase space representation of Gaussian modulated coherent states. Given the system is shot-noise limited, the overall quadrature variance at the receiver’s end is  $(T_{ch} \times \eta \times V_A + 1)N_0$ .

After quantum transmission stage, Bob announces which quadrature he measures for each incoming signal through an authenticated public channel, and Alice only keeps the corresponding data. If the observed noise is below certain threshold, they can further work out a secure key by performing reconciliation and privacy amplification. See more details in Section 3.

### C. Simultaneous quantum and classical communication protocol

It is straightforward to combine the above two communication protocols. In this simultaneous quantum and classical communication scheme, Alice encodes her classical binary bit  $m_A$  and Gaussian random numbers  $\{x_A, p_A\}$  on a coherent state  $|(x_A + e^{-im_A\pi}\alpha) + i(p_A + e^{-im_A\pi}\alpha)\rangle$ , as shown in Fig.1(c). Note in GMCS QKD based on homodyne detection, Bob measures a randomly chosen quadrature for each incoming signal. To achieve deterministic classical communication, the same classical bit  $m_A$  is encoded on both X and P quadrature. If het-

erodyne detection scheme is employed, then Alice only needs to encode  $m_A$  on one quadrature.

Assume Bob measures X-quadrature (P-quadrature) and his measurement results is  $x_R$  ( $p_R$ ). Bob first determines a classical binary bit  $m_B$  using the sign of  $x_R$  ( $p_R$ ), i.e., if  $x_R(p_R) > 0$ , then the value of  $m_B$  is assigned as “0”. Otherwise, the value of  $m_B$  is assigned as “1”. To extract the quantum information, Bob first displaces and rescales his measurement result based on the overall transmittance  $T_{ch} \times \eta$  and the value of  $m_B$  as follows

$$\begin{aligned} x_B &= \frac{x_R}{\sqrt{T_{ch} \times \eta}} + (2m_B - 1)\alpha \\ p_B &= \frac{p_R}{\sqrt{T_{ch} \times \eta}} + (2m_B - 1)\alpha \end{aligned} \quad (2)$$

Alice and Bob can further work out a secure key from raw keys  $\{x_A, x_B\}$  and  $\{p_A, p_B\}$ , just as in the case of conventional GMCS QKD.

Essentially, the states prepared by Alice are displaced Gaussian modulated coherent states, where the amount of displacement is determined by the classical bit  $m_A$ . Given a modulation variance  $V_A$ , the BER of classical communication can be reduced effectively by using a large displacement  $\alpha$ .

Next, we will show that the security proofs of the standard GMCS QKD can be applied to the new protocol. To illustrate the essential ideas, it is convenient to separate the classical channel from the quantum channel and allow Eve to have full access and control of the classical information, as shown in Fig.2 (a). In this picture, Bob performs a homodyne measurement on the incoming signal, then displaces his measurement results using classical information  $m_B$  (which could be provided by Eve). Equivalently, Bob could perform the displacement operation first, then perform the homodyne measurement, as shown in Fig.2 (b). Finally, we can move the displacement operation out of Bob’s secure station and let Eve to have full control of it, as shown in Fig.2 (c). Note the QKD model shown in Fig.2 (c) is the standard GMCS QKD, where Eve is allowed to manipulate the quantum signals transmitted through the channel at her will. So, the security of our new scheme is equivalent to that of the standard GMCS QKD.

In next section, we conduct numerical simulations to estimate the performance of the proposed scheme.

### III. SIMULATION RESULTS

To evaluate the performance of the proposed scheme, we conduct numerical simulations using realistic system parameters. Intuitively, since the quantum signal is superimposed on a relatively strong classical signal, we expect that noises from the classical channel will be coupled into the quantum channel. This will in turn reduce the QKD performance.

The assumptions adopted in the simulations are as follows. For classical communication, we assume the noise

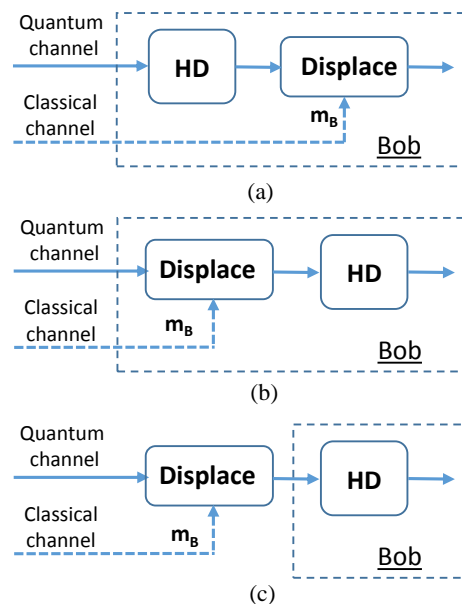


FIG. 2: Security models. HD—homodyne detection. (a) Our protocol; (b) A virtual QKD scheme equivalents to (a); (c) Standard GMCS QKD.

is dominated by the vacuum noise and the electrical noise of the homodyne detector. We further add in a constrain of  $BER \leq 10^{-9}$  in the classical channel. For QKD, we adopt the “realistic” model [9] where Eve cannot control the noise and loss inside Bob’s system. This “realistic” model has been widely adopted in long distance CV-QKD experiments [9, 10, 12, 23, 24].

We assume the communication channel between Alice and Bob is optical fiber with an attenuation coefficient of  $\gamma$ . The channel transmittance is given by

$$T_{ch} = 10^{-\frac{\gamma L}{10}} \quad (3)$$

where  $L$  is the fiber length.

Given the electrical noise of the homodyne detector is  $\nu_{el}N_0$ , Eq.(1) becomes

$$BER = \frac{1}{2} \text{erfc} \left( \frac{\sqrt{T_{ch}\eta}\alpha}{\sqrt{2(T_{ch}\eta V_A + 1 + \nu_{el})N_0}} \right) \quad (4)$$

where  $V_A$  is the variance of Gaussian modulation.

To achieve  $BER = 10^{-9}$  in the classical channel, we can show that (4) requires

$$\alpha = 4.24 \times \frac{\sqrt{T_{ch}\eta V_A + 1 + \nu_{el}}}{\sqrt{2T_{ch}\eta}} \quad (5)$$

Under the assumption of  $\alpha^2 \geq V_A + 1$ , the impact of the classical signal on the quantum channel can be estimated by an excess noise term

$$\varepsilon_c = \alpha^2 \times \sigma_\phi \quad (6)$$

where  $\sigma_\phi$  is the phase noise variance of the communication system, which may include both the phase noise

between the signal and the LO, and other modulation errors.

The secure key rate, under the optimal collective attack, in the case of reverse reconciliation, is given by [24]

$$R = fI_{AB} - \chi_{BE} \quad (7)$$

where  $I_{AB}$  is the Shannon mutual information between Alice and Bob;  $f$  is the efficiency of the reconciliation algorithm;  $\chi_{BE}$  is the Holevo bound of the information between Eve and Bob. We remark that more advanced security proofs of CV-QKD have been developed [25]. Here, we adopt the security analysis given in [24] to facilitate the comparison with previous experimental results.

The mutual information between Alice and Bob is given by

$$I_{AB} = \frac{1}{2} \log_2 \frac{V + \chi_{tot}}{1 + \chi_{tot}} \quad (8)$$

The Holevo bound of the information between Eve and Bob is given by [24]

$$\chi_{BE} = \sum_{i=1}^2 G\left(\frac{\lambda_i - 1}{2}\right) - \sum_{i=3}^5 G\left(\frac{\lambda_i - 1}{2}\right) \quad (9)$$

where  $G(x) = (x + 1)\log_2(x + 1) - x\log_2 x$

$$\lambda_{1,2}^2 = \frac{1}{2} \left[ A \pm \sqrt{A^2 - 4B} \right] \quad (10)$$

where

$$A = V^2(1 - 2T_{ch}) + 2T_{ch} + T_{ch}^2(V + \chi_{line})^2 \quad (11)$$

$$B = T_{ch}^2(V\chi_{line} + 1)^2 \quad (12)$$

$$\lambda_{3,4}^2 = \frac{1}{2} \left[ C \pm \sqrt{C^2 - 4D} \right] \quad (13)$$

where

$$C = \frac{A\chi_{hom} + V\sqrt{B} + T_{ch}(V + \chi_{line})}{T_{ch}(V + \chi_{tot})} \quad (14)$$

$$D = \sqrt{B} \frac{V + \sqrt{B}\chi_{hom}}{T_{ch}(V + \chi_{tot})} \quad (15)$$

$$\lambda_5 = 1 \quad (16)$$

System parameters in the above equations are defined as follows.

- (a)  $V = V_A + 1$ , where  $V_A$  is the variance of Gaussian modulation.
- (b) The total noise referred to the channel input  $\chi_{tot} = \chi_{line} + \frac{\chi_{hom}}{T_{ch}}$ , where  $T_{ch}$  is the channel transmittance as defined in (3).

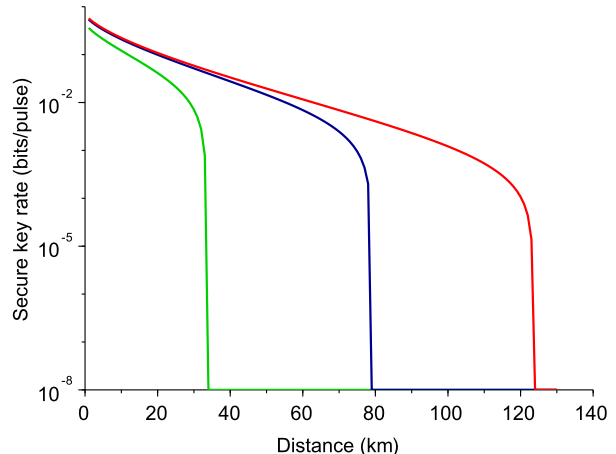


FIG. 3: Simulation results based on security analysis given in [24]. Simulation parameters:  $\alpha = 0.2$  dB/km,  $\nu_{el} = 0.1$ ,  $V_A = 4$ ,  $\eta = 0.5$ ,  $f = 0.95$ , and  $\sigma_\phi = 0.001$  (green), 0.0001 (blue), 0.00001 (red).

- (c) The total channel-added noise referred to the channel input  $\chi_{line} = \frac{1}{T_{ch}} - 1 + \varepsilon_c$ . Here we assume that  $\varepsilon_c$  dominates the excess noise outside of Bob's system.
- (d) The detection-added noise referred to Bob's input  $\chi_{hom} = [1 - \eta + \nu_{el}]/\eta$ , where  $\nu_{el}$  and  $\eta$  are detector noise and efficiency, respectively.

We conduct numerical simulations for different phase noise variances  $\sigma_\phi = (0.001, 0.0001, 0.00001)$ . Other simulation parameters are:  $\alpha = 0.2$  dB/km,  $\nu_{el} = 0.1$ ,  $\eta = 0.5$ ,  $f = 0.95$ , and  $V_A = 4$ . Fig. 3 shows the simulation results. The performance of the proposed scheme is heavily dependent on the phase noise of the system. Under a realistic phase noise level of  $\sigma_\phi = 0.001$  [24], secure key can be distributed over 30km optical fiber under the constrain of  $BER = 10^{-9}$  in the classical communication channel.

#### IV. DISCUSSION

One major roadblock to the wide applications of QKD is the high implementation cost. Conventionally, dedicated hardware are required to implement QKD protocols. In this paper, we show that by using optical coherent detection, classical communication and QKD can be implemented simultaneously on the same platform.

Our simulation results suggest that the QKD performance is largely determined by the phase noise of the system. To extend the distance of QKD, sophisticate phase stabilization scheme may be required.

Note in our study, an uncoded BPSK scheme is assumed for classical communication. The excess noise due

to classical channel is proportional to the photon number per bit, as shown in (6). By applying powerful forward-error-correction coding in classical channel, the required photon number per bit required to achieve a given BER can be further reduced [15]. This will in turn reduce the excess noise in QKD and lead to a better performance.

It is conceivable that in future coherent optical communication network, QKD is operated in the background of classical communication. This may allow us to generate secure key with negligible cost. We expect the simultaneous quantum and classical communication scheme presented here will have great impact on the practical application of QKD.

This work was performed at Oak Ridge National

Laboratory (ORNL), operated by UT-Battelle for the U.S. Department of Energy under Contract No. DE-AC05-00OR22725. The U.S. Government retains and the publisher, by accepting the article for publication, acknowledges that the U.S. Government retains a non-exclusive, paid-up, irrevocable, world-wide license to publish or reproduce the published form of this manuscript, or allows others to do so, for U.S. Government purposes. The Department of Energy will provide public access to these results of federally sponsored research in accordance with the DOE Public Access Plan (<http://energy.gov/downloads/doe-public-access-plan>). The authors acknowledge support from ORNL laboratory directed research and development program.

- 
- [1] C. H. Bennett and G. Brassard, in *Proceedings of IEEE International Conference on Computers, Systems and Signal Processing* (IEEE Press, New York, 1984), pp. 175-179.
- [2] A. K. Ekert, *Phys. Rev. Lett.* **67**, 661 (1991).
- [3] N. Gisin, G. Ribordy, W. Tittel, and H. Zbinden, *Rev. Mod. Phys.* **74**, 145 (2002).
- [4] V. Scarani, H. Bechmann-Pasquinucci, N. J. Cerf, M. Dušek, N. Lütkenhaus, and M. Peev, *Rev. Mod. Phys.* **81**, 1301 (2009).
- [5] H.-K. Lo, M. Curty, and K. Tamaki, *Nat. Photonics* **8**, 595 (2014).
- [6] Y. Zhao, B. Qi, X. Ma, H.-K. Lo, and L. Qian, *Phys. Rev. Lett.* **96**, 070502 (2006).
- [7] T. C. Ralph, *Phys. Rev. A* **61**, 010303(R) (1999).
- [8] M. Hillery, *Phys. Rev. A* **61**, 022309 (2000).
- [9] F. Grosshans, G. V. Assche, J. Wenger, R. Brouri, N. J. Cerf, and Ph. Grangier, *Nature* **421**, 238 (2003).
- [10] P. Jouguet, S. Kunz-Jacques, A. Leverrier, Ph. Grangier, and E. Diamanti, *Nat. Photonics* **7**, 378 (2013).
- [11] B. Qi, W. Zhu, L. Qian, and H.-K. Lo, *New J. Phys.* **12**, 103042 (2010).
- [12] R. Kumar, H. Qin, and R. Alléaume, *New J. Phys.* **17**, 043027 (2015).
- [13] B. Heim, C. Peuntinger, N. Killoran, I. Khan, C. Wittmann, Ch. Marquardt, and G. Leuchs, *New J. Phys.* **16**, 113018 (2014).
- [14] K. Kikuchi, *IEEE J. Lightw. Technol.* **34**, 157 (2016).
- [15] M. L. C. Stevens, D. O. Robinson, B. S. Boroson, D. M. Kachelmyer, and A. L. Kachelmyer, *Opt. Exp.* **16**, 10412 (2008).
- [16] Y.-B. Zhao, M. Heid, J. Rigas, and N. Lütkenhaus, *Phys. Rev. A* **79**, 012307 (2009).
- [17] A. Leverrier and Ph. Grangier, *Phys. Rev. Lett.* **102**, 180504 (2009).
- [18] A. Marie and R. Alléaume, arXiv:1605.03642 (2016).
- [19] B. Qi, P. Lougovski, R. Pooser, W. Grice, and M. Bobrek, *Phys. Rev. X* **5**, 041009 (2015).
- [20] D. B. S. Soh, C. Brif, P. J. Coles, N. Lütkenhaus, R. M. Camacho, J. Urayama, and M. Sarovar, *Phys. Rev. X* **5**, 041010 (2015).
- [21] D. Huang, P. Huang, D. Lin, C. Wang, and G. Zeng, *Opt. Lett.* **40**, 3695 (2015).
- [22] C. Weedbrook, A.M. Lance, W.P. Bowen, T. Symul, T.C. Ralph, and P.K. Lam, *Phys. Rev. Lett.* **93**, 170504 (2004).
- [23] B. Qi, L.-L. Huang, L. Qian, and H.-K. Lo, *Phys. Rev. A* **76**, 052323 (2007).
- [24] J. Lodewyck, M. Bloch, R. García-Patrón, S. Fossier, E. Karpov, E. Diamanti, T. Debuisschert, N. J. Cerf, R. Tualle-Brouri, S. W. McLaughlin, and Ph. Grangier, *Phys. Rev. A* **76**, 042305 (2007).
- [25] A. Leverrier, *Phys. Rev. Lett.* **114**, 070501 (2015).